



Monitoring of Deep Groove Ball Bearing Defects Using the Acoustic Emission Technology

Mohamed El-Shaib^{a*}, Omar Keshk^b, Mohamed Shehadeh^c

^{a,b,c}*Arab Academy for science technology and maritime transportation, Alexandria, Egypt*

^a*Email: Mohamed.elshaib@aast.edu*

^b*Email: omar_keshk87@outlook.com*

^c*Email: ezzfahmy@aast.edu*

Abstract

One of the essential components in rotating machinery are Rolling element bearings and their failure proved to be one of the most common reasons behind machine breakdown. Acoustic Emission (AE), a passive listening technique, has evolved as a significant opportunity to diagnose and monitor the mechanical integrity of rolling element bearings. The investigation reported in this paper mainly focuses on the application of the AE technology for detecting the defect on a radially loaded bearing. In order to undertake this task, a special purpose test-rig was designed so that defect could be seeded onto the outer race of a test bearing using an electrical engraver. By applying varying rotating speed and radial load, twenty tests were carried out. The structure mechanism allows locating an AE sensor directly on the bearing outer race. The AE wave signal has been analyzed in time and frequency domain. It was concluded that the AE can provide good indications of bearing defects. Moreover, it has been noted that the amplitude, absolute energy, and RMS provided indications of bearing condition.

Keywords: Acoustic emission; bearing defect diagnosis; condition monitoring.

* Corresponding author.

1. Introduction

Rotating machinery is widely used and is key equipment in many industries. The importance of condition monitoring and fault diagnosis of such equipment has been extensively recognized by both the industry and research community. Due to their low cost and reliability, rolling element bearings are among the essential components used in rotating machinery. However, the correct condition of the bearings is required to guarantee the normal and safe running of the machines. Any failures in the bearings such as fatigue cracks, pitting, spalling, etc., must be detected quickly. Otherwise they may cause malfunctions or even a catastrophic accident [1].

During operation, intermittent or continuous monitoring of machines is an attractive opportunity for maintenance based on the actual condition of a machine rather than a predefined, fixed schedule. If the condition of components can be determined during operation, maintenance can be performed only when needed [2]. AE was originally developed for non-destructive testing of static structures [3, 4], however, it has been extended to health monitoring of rotating machines and bearings [5]. It offers the advantage of earlier defect detection in comparison to vibration analysis.

Nevertheless, limitations in the successful application of AE technique for monitoring bearings have been partly caused by the difficulty in processing, interpreting and classifying the acquired data [6, 7].

The application of the high-frequency AE technique in condition monitoring of rotating machinery has been growing over recent years. This is particularly true for bearing defect diagnosis and seal rubbing [8-13]. Several studies have been conducted to analyze the AE response of defective bearings. Shiroishi and his colleagues [14] investigated defect detection methods for rolling element bearings through sensor signature analysis; they compared vibration and AE on seeded defective bearings. They noted that the peak ratio was the most reliable indicator of the presence of a localized defect with the RMS. Reference [15] employed AE for bearing defect identification on various sized bearings and rotational speeds. The defects in the roller and inner race of the bearings were simulated by the spark erosion method. On one hand, it was concluded that AE counts increased with the increasing speed for damaged and undamaged bearings. On the other hand, an increase in load did not result in any significant changes in AE counts for both damaged and undamaged bearings. To ascertain the most appropriate threshold level for AE count diagnosis in rolling element bearings, an investigation was undertaken by Reference [7]. Results demonstrated that the values of AE maximum amplitude did correlate with the increasing speed, but not with load and defect size. In addition, Reference [16] simulated two types of defects on the inner and outer races of spherical roller bearing. The seeded fault was a uniform surface line defect that was accomplished with an engraving machine. The test-rig was operated at three different rotational speeds and three radial load cases. It was concluded that the AE counts increased with the increasing speed, irrespective of the threshold level, and that RMS values increased with the increasing load, speed and defect size. Moreover, in their work, Al-Dossary and his colleagues [17], presented the application of the AE technology for characterizing the defect sizes on a radially loaded split Cooper cylindrical roller bearing. An experimental test-rig was designed so that defects of varying sizes could be seeded on to the outer and inner races of a test bearing. The test rig was run at the two speeds and three radial loads. It was demonstrated that the increase in defect size resulted in an increase in levels of AE energy for outer and inner race seeded defects. Furthermore, He and his colleagues [1] used a

deep ditch ball-bearing, as a test bearing. Three load cases were applied and two rotating speeds of the test rig were chosen. They proved that a constant load applied to the bearing has no obvious influence on the AE parameters, but the rotating speed has a strong influence on the AE parameters for almost every running condition. The specifications of the test bearing used in the experiment are tabulated in Table 1.

Table 1: Test bearing specifications

FEATURE	DETAIL
BEARING TYPE	DEEP GROOVE BALL BEARING OF TYPE ZKL 6406
NUMBER OF BALLS	7
OUTER DIAMETER	90 MM
INNER DIAMETER	30 MM
WEIGHT	0.725 KG

1. Test rig

Figure 1 shows an actual test rig setup, which consists of the following: an asynchronous motor (1.1 kW), a 30mm diameter shaft supported on two deep groove ball bearings of type URB 6006, a rotor-bearing unit, a loading unit, test bearing (see Figure 2), and a hub attached to the outer race of the test bearing. This housing was assembled to allow for the locating of the AE sensor straight onto the race. The speed of the rig can be adjusted easily by a variable frequency drive handle that ranges between 0 up to 1500 rpm. The radial load is applied to the test bearing by a power screw connected to a pulley and a belt system as shown in the same figure. The test bearing was lubricated by a jet of Mobil ATF 320 oil. Rubber sheets have also been provided under the system for the purpose of vibration isolation (i.e. eliminate noises).

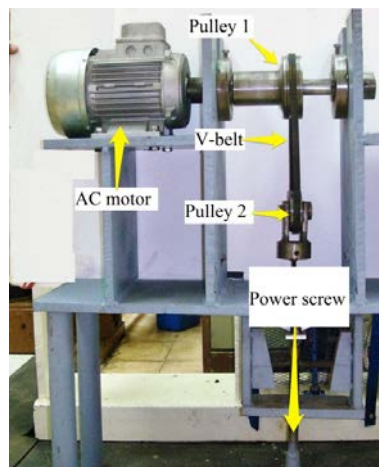


Figure 1: Test rig

2. Experimental procedure

Twenty sets of AE data were recorded, ten of them for defect free condition and for the outer race defect condition. The procedure for recording the data simply involved over a 30-second period for each simulation. This was done in order to provide acceptable reliable test signal on the robustness of specific AE characteristic parameters for the diagnosis of operational bearings. An electrical engraver with a carbide tip was used to seed a simulated seeded defect onto the outer race of the bearing artificially as exemplified in figure 3. Shiroishi and his colleagues [11] noted that the AE sensor was not sensitive to the inner race. Initially, a defect was seeded on the outer race just beside the location where the AE sensor was mounted. Two load cases and five rotating speeds of the test rig were considered (see Table 2). The AE parameters measured for diagnosis in this particular investigation were amplitude, RMS, and absolute energy. Figure 4 demonstrates the experimental procedure steps.

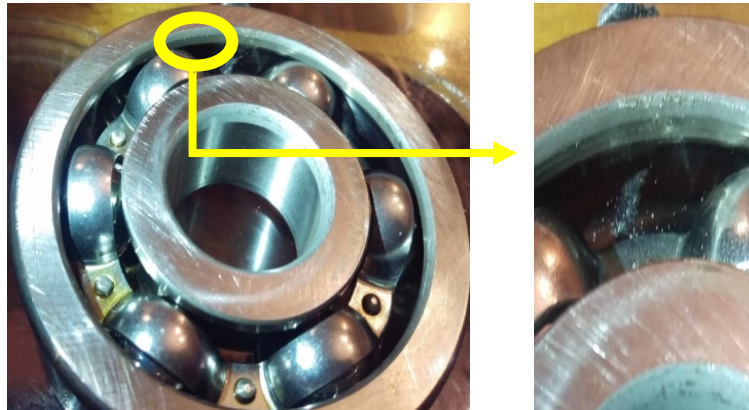


Figure 2: Typical test Bearing

Figure 3: Outer race seeded defect

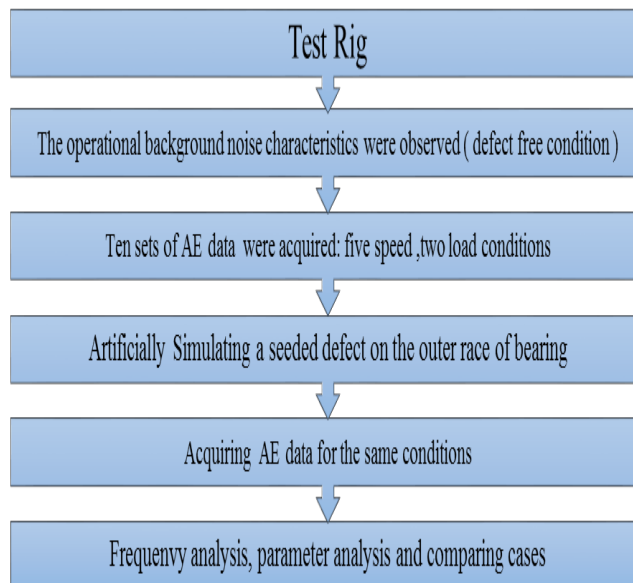


Figure 4: Experimental procedure

Table 2: Load and speed running conditions

LOAD	NO LOAD					350 N				
SPEED (RPM)	300	600	900	1200	1500	300	600	900	1200	1500

The diameter of the sensor was 19 mm, while the thickness of the test bearing races was 9 mm. accordingly, a wave guide has been used to be a coupling between the sensor and the bearing races. The wave guide was designed from stainless steel in a conical shape that has two diameters of 21 mm and 7mm, and length of 20 mm, as shown in Figure 5. Further, Figure 6 shows the effect of the cone on the AE signal that has been measured by a Pencil-Lead Breakage Test (PLB), a Hsu-Nielsen source [3]. The pencil lead was broken on the specimen surface and the sensor was placed on the same surface directly which was mounted on the wave guide. The distance between the source and the sensor was constant in all experiments. The experiment was repeated five times, and when the amplitude of AE signal was averaged, the attenuation was measured and it was observed that the used wave guide made an attenuation of 0.3 dB.

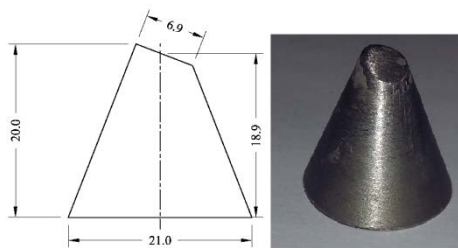


Figure 5: Wave guide dimensions in mm.

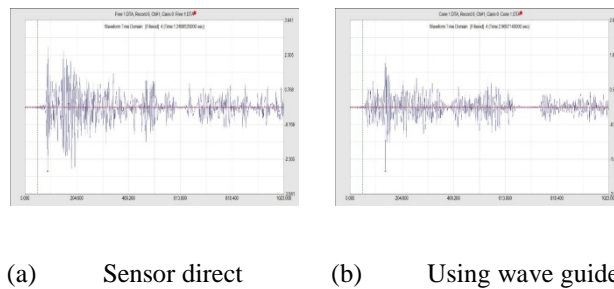


Figure 6: Time domain signals before and after wave guide

3. Results and discussion

The analysis of the acquired AE signal has been carried out in frequency and time domains.

3.1 Time domin analysis

The waveform signal was filtered using a high pass filter (Chebyshev) 100 kHz to eliminate motor effects. The raw data signal (Waveform) is shown in Figures 7 and 8, before and after seeded defect as well as with and without loads.

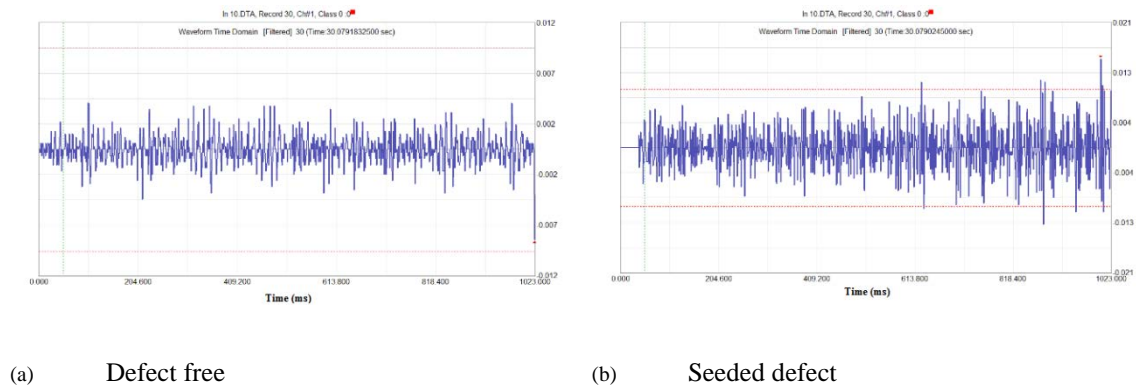


Figure 7: Time domain waveform (Raw data) at 300 rpm at no load

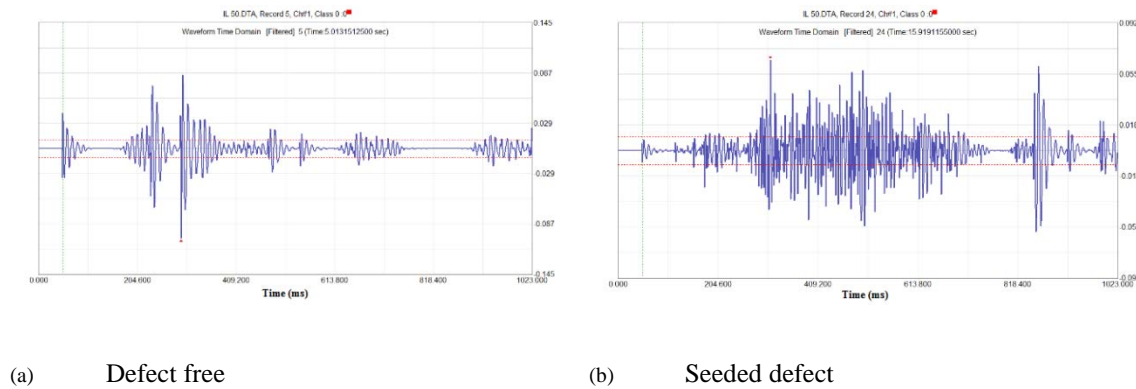


Figure 8: Time domain waveform (Raw data) at 1500 rpm at load of 350 N

- Ae rms:

The Root Mean Square (RMS) is an electrical engineering power term defined as the rectified, time-averaged signal, measured on a linear scale and reported in volts. Keeping into consideration, the RMS value gives the intensity of the AE signature. Recently, this parameter is intensively used for signal analysis. For each test performed (20 in total), AE data was acquired for 30 seconds. AE measurement results are discussed. Additionally, the guidelines for interpreting the AE measurement results for prediction of the seeded defect on the outer race of test bearing are also deliberated. A clear relationship between the RMS level, rotational speed and radial load has been reported. For all test conditions, results clearly indicated a rise in RMS values with increasing rotational speed. Results from seeded defect indicated that RMS values increased with the increasing speed. In addition, at fixed rotational speeds, there was evidence to propose that increasing the load also resulted in an increase of RMS. The RMS values, at no load, are increased by more than 40% at speeds of 1200 and 1500 rpm.

Also, at load of 350 N, the increasing in values was clearly observed from a speed of 900 rpm along with higher speeds of 1200 and 1500 rpm. This is clearly demonstrated in Figure 11.

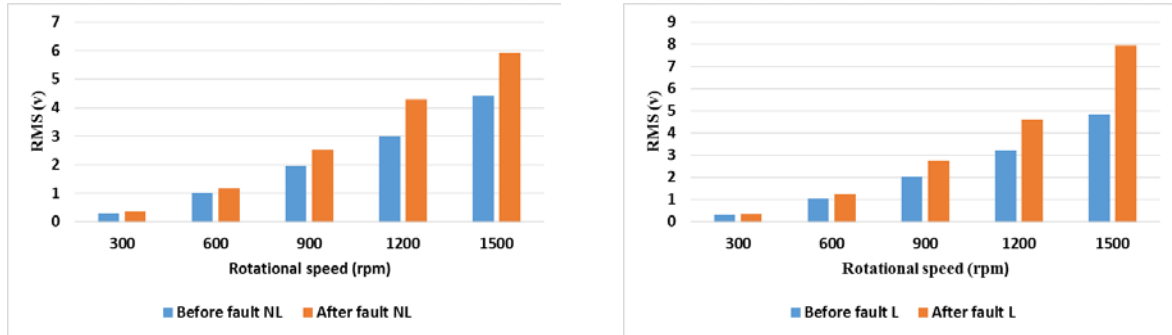


Figure 9: Average RMS (a) No load, (b) 350 N load

- AE Absolute Energy:

The absolute energy is a measure of the true energy. It is derived from the integral of the squared voltage signal divided by the reference resistance (10 k-ohms) over the duration of the AE signal. The unit for absolute energy is atto-joules (10^{-18} joules). This energy is directly proportional to the electrical energy of the AE signal in the measured bandwidth by a constant of system electric impedance which, in this instance, was 10kΩ. The absolute energy values were compared at varying speeds and load conditions for defect free and seeded defect. It was deduced that absolute energy values increased with the increasing speed, although the increase with load was observed at 900, 1200, and 1500 rpm. A seeded defect condition resulted in an increase in absolute energy values which was clearly observed only at speeds of 1200 and 1500 rpm. Figure 12 explains that.

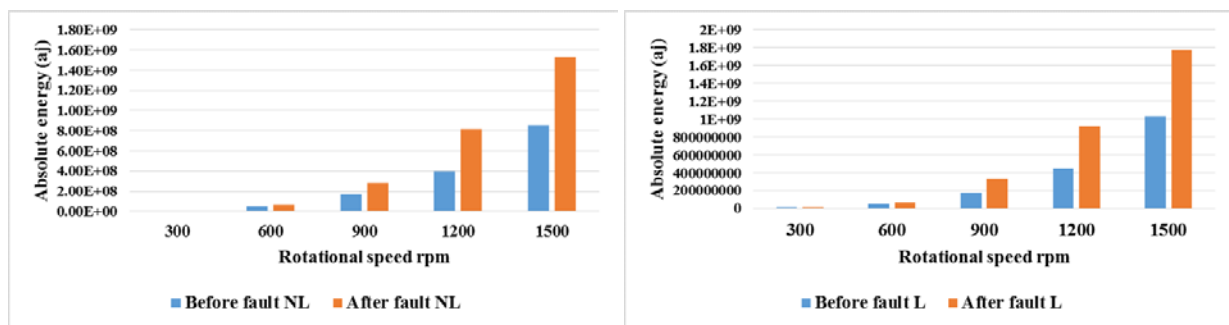


Figure 10: Average Absolute energy (a) No load, (b) 350 N load

- AE signal amplitude:

Amplitude (A) is the greatest measured voltage in a waveform and is measured in decibels (dB). This is an important parameter in AE inspection because it determines the delectability of the signal. Since signals with amplitudes are below the operator-defined, the minimum threshold will not be recorded. It was noted that AE average amplitude increased by the increasing speed and load, see Figure 13. It was also evident that AE amplitude increased from fault free condition to the seeded defect.

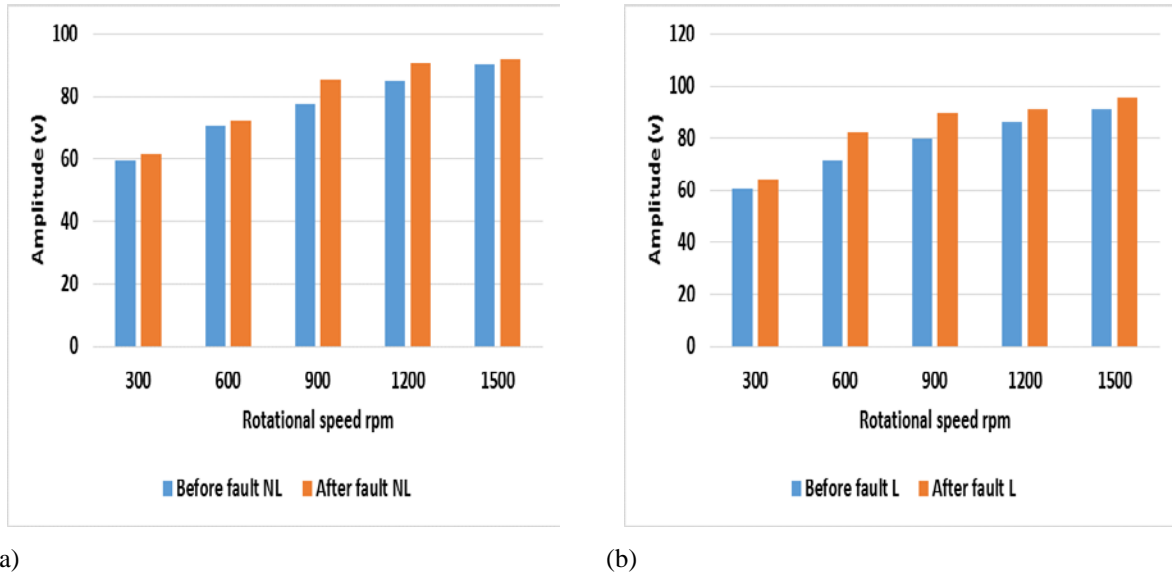


Figure 11: Average amplitude (a) No load, (b) 350 N load

In general, AE RMS could be used to identify the faults over a wide range of speeds from 600 to 1500 rpm, as shown in Table 3. However, as explained in Table 4, the sharp rise in the values of absolute energy for the defect tested indicates that this may serve as a clear parameter for incipient fault detection in bearings at speeds above 900 rpm. In spite of the fact that the signal amplitude has a percentage difference between defect free and seeded defect, this difference is small in comparison to RMS and absolute energy results (see Table 5). For identifying bearing faults, the bearing should be tested at speeds higher than 900 rpm in order to make results clearer. Parameters percentage difference was calculated by using Equation (1).

$$\frac{(\text{Parameter average value})_{\text{After fault}} - (\text{Parameter average value})_{\text{Before fault}}}{(\text{Parameter average value})_{\text{Before fault}}} * 100\% \quad \text{Equation (1)}$$

Table3: RMS percentage differences

ROTATIONAL SPEED	300 RPM	600 RPM	900 RPM	1200 RPM	1500 RPM
NO LOAD	18.4%	25.8%	28.24%	43.1%	47.3%
350 N	29.3%	38.78%	47.48%	53.59%	64.44%

Table 4: Absolute energy percentage differences

ROTATIONAL SPEED	300 RPM	600 RPM	900 RPM	1200 RPM	1500 RPM
NO LOAD	34.9%	40.4%	63.5%	78.7%	106%
350 N	37.6%	42.1%	74.9%	80.2%	108%

Table 5: AE Amplitude percentage differences

ROTATIONAL SPEED	300 RPM	600 RPM	900 RPM	1200 RPM	1500 RPM
NO LOAD	2.4%	2.69%	6.25%	6.42%	8.43%
350 N	2.82%	5.98%	7.07%	7.54%	8.7%

3.2 AE Frequency Analysis

The frequency spectra of the hit with the highest energy were recorded during all running conditions. Frequency analysis provided indications of bearing defect. While the range of signal frequency increased from 150 kHz for defect free condition to be about 300 kHz after the outer race defect for all speed and load conditions. Therefore, it can be used as a finger print to the presence of faults on the bearing’s races. For example, in this case study, the frequency range is increased higher than 200 kHz, which is indicated to faulty bearing, see Figures 9 and 10.

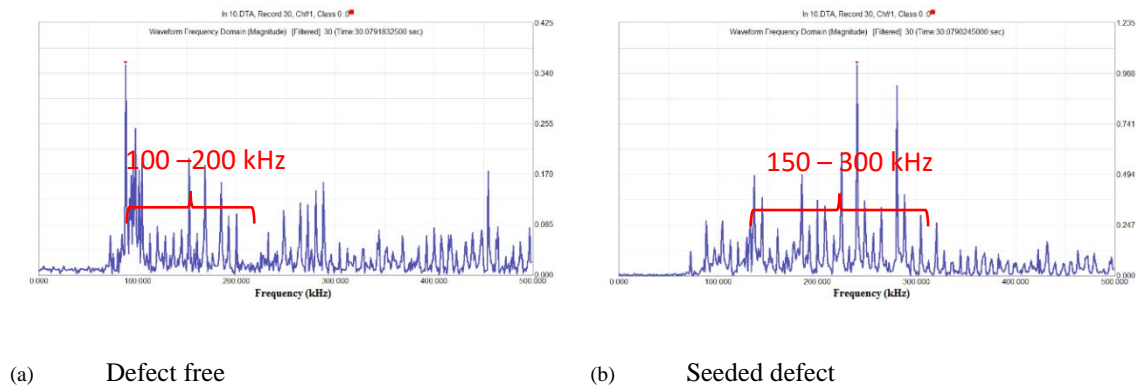


Figure 12: Frequency analysis (FFT magnitude) at 300 rpm at no load

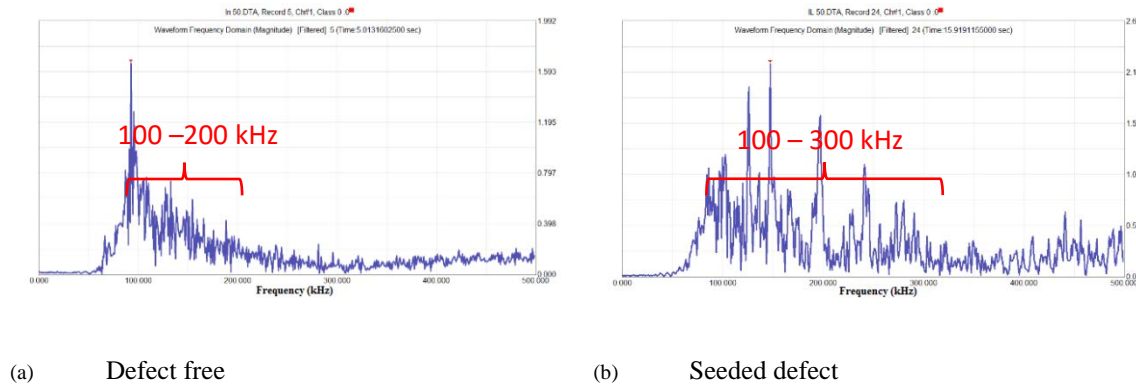


Figure 13: Frequency analysis (FFT magnitude) at 1500 rpm at load of 350 N

4. Conclusion

The utility of the AE method for defect detection in rolling element deep groove ball bearings has been examined. AE parameters, such as RMS, amplitude, and absolute energy, were measured for running conditions of radial load and rotating speed, these parameters have been authorized as proposed techniques for spotting bearing damage. The results of AE parameter analysis validate that all the mentioned above parameters improved after outer race defect. Moreover, the radial load also has some influence on the AE parameters. However, the rotating speed has an impact on the AE parameters for almost every running condition.

Therefore, from the physical meaning of AE parameters, it was concluded that the rotating speed has a powerful influence on the AE parameters under most running conditions of the bearing. The radial load has little evident effect on the generation of AE. Generally, in order to motivate good AE signal for monitoring faults of the bearing, the rotating speed should be increased in order to enhance the results.

References

- [1] He, Y., Zhang, X., and Friswell, M., 2009, Defect Diagnosis for Rolling Element Bearings Using Acoustic Emission. *Vibration and Acoustics*, 131 (061012), 1-10.
- [2] Ruuska, M., and Andersson, P.H., 2003, SPINDLE BEARING MONITORING USING ACOUSTIC EMISSION. XVII IMEKO World Congress, Dubrounik, Croatia.
- [3] Elforjani, M., and Mba, D., 2010, Accelerated natural fault diagnosis in slow speed bearings with Acoustic Emission. *Engineering Fracture Mechanics*, 77, 112-127.
- [4] Aboali, A., El-Shaib, M., Sharara, A., Shehadeh, M., 2014, Screening for welding defects using acoustic emission technique , *Advanced Materials Research*, 1025-1026, pp. 7-12.
- [5] Naguib, A., El-Shaib, M., Adel, M., Shehadeh, M., 2015, Predicting the residual stresses in steel t-section beams using acoustic emission technique. *International Review of Mechanical Engineering*, 9 (2).
- [6] Morhain, A., and Mba, D., 2003, Bearing defect diagnosis and acoustic Emission. *Engineering Tribology*, 217 (4), 257-272.
- [7] Shehadeh, M., Shahata, A.I., El-Shaib, M., Osman, A., 2013, Numerical and experimental investigations of erosion-corrosion in carbon-steel pipelines, 8 (11), pp 1217-1231.
- [8] Siores, E. and Negro, A.A., 1997. Condition monitoring of a gear box using acoustic emission testing. *Material Evaluation*, 55 (2), 183-187.
- [9] Mba, D. and Bannister, R.H., 1999. Condition monitoring of low-speed rotating machinery using stress waves: Part 1 and Part 2. *Journal of Process Mechanical Engineering*, 213(3), 153-185.
- [10] Mba, D., Cooke, A., Roby, D. and Hewitt, G., 2003. Opportunities offered by acoustic emission for shaft-seal rubbing in power generation turbines; a case study. Conference sponsored by the British Institute of NDT. International Conference on Condition Monitoring, Oxford, UK.
- [11] Kim, Y.H., Tan, A.C.C., Mathew, J., Kosse, V. and Yang, B.S. 2007. A comparative study on the application of acoustic emission technique and acceleration measurements for low speed condition monitoring, 12th Asia-Pacific Vibration Conference, Hokkaido Univ. Japan.
- [12] Gu, D.G, Kim, J.G., An, Y.S. and Choi, B.K., 2011. Detection of faults in gearboxes using acoustic

- emission signal. *Journal of Mechanical Science and Technology*, 25 (5), 1279-1286.
- [13] Toutountzakis, T. and Mba, D., 2003. Observations of acoustic emission activity during gear defect diagnosis. *NDT&E International*, 36 (7), 471–477.
- [14] Shiroishi, J., Li, Y., Liang, S., Kurfess, T., and Danyluk, S., 1997, Bearing condition diagnostics via vibration and acoustic emission measurements. *Mechanical Systems and Signal Processing*, 11 (5), 693-705.
- [15] Choudhury, A., and Tandon, N., 2000, Application of acoustic emission technique for the detection of defects in rolling element bearings. *Tribology International*, 33, 39–45.
- [16] Mba, D., 2003, Acoustic Emissions and monitoring bearing health. *Tribology Transactions*, 46 (3), 447-451.
- [17] Al-Dossary, S., Hamzah, R.I., and Mba, D., 2009, Observations of changes in acoustic emission waveform for varying seeded defect sizes in a rolling element bearing. *Applied Acoustics* 70, 58–81.